Tectonophysics 851 (2023) 229772

Contents lists available at ScienceDirect

Tectonophysics

journal homepage: www.elsevier.com/locate/tecto

# Active tectonics in the Calabrian Arc: Insights from the Late Miocene to Recent structural evolution of the Squillace Basin (offshore eastern Calabria)

M. Corradino [a,b], D. Morelli [c], S. Ceramicola [d], L. Scarfì [e], G. Barberi [e], C. Monaco [a,e,f], F. Pepe [b,*]

[a] Department of Biological, Geological and Environmental Sciences, University of Catania, Catania, Italy
[b] Department of Earth and Marine Sciences, University of Palermo, Palermo, Italy
[c] Department for the Earth, Environment and Life Sciences, University of Genoa, Genoa, Italy
[d] OGS - Istituto Nazionale di Oceanografia e di Geofisica Sperimentale, Trieste, Italy
[e] Istituto Nazionale di Geofisica e Vulcanologia, Osservatorio Etneo, Catania, Italy
[f] CRUST - Interuniversity Center for 3D Seismotectonics With Territorial Applications, Italy

ARTICLE INFO

*Keywords:*
Active tectonics
Strike-slip tectonics
Calabrian Arc (Italy)
Ionian Sea
Tyrrhenian Sea

ABSTRACT

The Calabrian Arc represents one of the most active sectors of the upper plate of the Tyrrhenian-Ionian subduction system. This research aims to reconstruct the evolution of the Squillace Basin (Ionian offshore of the Calabrian Arc) from the Late Miocene to Recent times and recognise active shallow and deep structures using a multiscale approach. The latter is based on interpreting high-penetration and high-resolution seismic reflection profiles, calibrated with well-log data coupled with bathymetric data and the distribution of instrumental earthquakes. Data highlight three steps in the evolution of the Squillace Basin. A Late Miocene extensional event led to the formation of WNW-ESE oriented horst and half-graben structures. During the Pliocene, deformation was localised in the central and northern sectors of the basin and expressed by a WNW-ESE oriented strike-slip fault and NW-SE normal to trastensional faults, respectively. A transpressional event started in the Early Pleistocene, causing the positive inversion of deep (> 3 km) extensional faults and the formation of NW-SE to WNW-ESE oriented transpressional/reverse faults and related anticlines. The kinematics of these faults agree with the NW-SE oriented left-lateral Albi-Cosenza, Lamezia-Catanzaro and Petilia-Sosti crustal fault zones developed in north Calabria. The results of this work suggest that the transpressional structures in the northwestern sector of the basin likely represent the offshore prolongation of the Albi-Cosenza fault zone. NW-SE to WNW-ESE trending, shallow (<2 km) high-angle normal faults offset the younger deposits. Their depth and direction indicate that these faults are secondary structures formed in the extrados of the anticlines associated with the transpressional faults. The distribution of earthquakes shows events with M > 3 and depth <15 km located in the hanging wall of transpressional faults. The integrated data suggest that these structures are active and probably responsible for the major earthquakes that affected the Ionian offshore.

## 1. Introduction

The Calabrian Arc developed in the frame of the Tyrrhenian-Ionian subduction system since the Neogene by the sinking of the Ionian oceanic lithosphere below the European plate (Fig. 1a-c, Faccenna et al., 2001). Lithospheric discontinuities and regional-scale crustal shear zones control the tectono-sedimentary evolution of the Calabrian Arc and its offshore. Polyphase subsidence and inversion tectonics in basins developed along the Calabrian Arc and its offshore testify rapid changes in time and space of direction and magnitude of stress induced by the frontal accretion of the Apulian and Ionian domains (e.g. Brutto et al., 2016; Corradino et al., 2021; Loreto et al., 2013).

The Catanzaro Trough and its eastern offshore prolongation, the Squillace Basin, belongs to the forearc region of the Tyrrhenian-Ionian subduction system and separates the northern and southern Calabrian Arc (Fig. 1b). Literature data highlight that this area is affected by a complex interaction between 1) lateral and trench-parallel slab tearing (Maesano et al., 2017; Neri et al., 2009; Rosenbaum et al., 2008; Scarfì

* Corresponding author.
*E-mail address:* fabrizio.pepe@unipa.it (F. Pepe).

https://doi.org/10.1016/j.tecto.2023.229772
Received 8 August 2022; Received in revised form 10 February 2023; Accepted 23 February 2023
Available online 27 February 2023

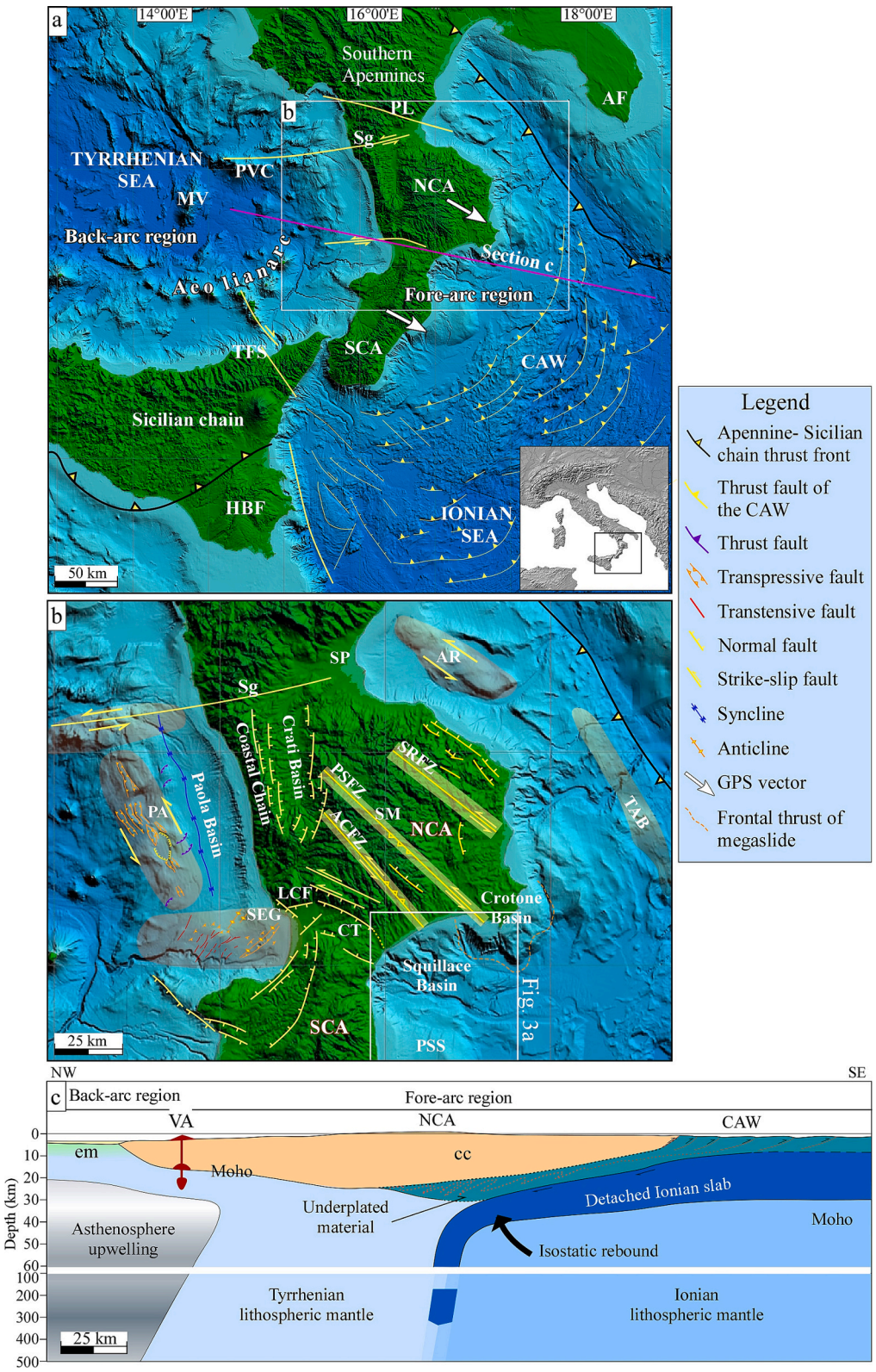


**Fig. 1.** (a) Schematic tectonic map of the Tyrrhenian-Ionian subduction system. Inset shows the location of the panel a. (b) Schematic map of the major tectonic structures of the Calabrian Arc (modified from Brutto et al., 2016; Corradino et al., 2020, 2021; De Ritis et al., 2019; Ferranti et al., 2014; Monaco and Tortorici, 2000; Tansi et al., 2007; Van Dijk, 1991; Van Dijk et al., 2000; Volpi et al., 2017). The white rectangle indicates the study area. (c) Schematic cross-section showing the lithospheric structure across the backarc and forearc regions of the Tyrrhenian-Ionian subduction system (modified from Corradino et al., 2020; 2022). Purple line in panel a is the section trace. Abbreviations: ACFZ, Albi-Cosenza fault zone; AF, Apulian foreland; AR, Amendolara ridge; CAW, Calabrian accretionary wedge; cc, continental crust; CT, Catanzaro Trough; em, exhumed mantle; HBF, Hyblean foreland; LCF, Lamezia- Catanzaro fault system; MV, Marsili volcano; NCA, northern Calabrian Arc; PA, Paola anticline; PL, Pollino; PSFZ, Petilia-Sosti fault zone; PSS, Punta Stilo Swell; PVC, Palinuro volcano complex; SCA, southern Calabrian Arc; SEG, Sant'Eufemia Gulf; Sg, Sangineto line; SM, Sila Massif; SP, Sibari Plain; SRFZ, S. Nicola-Rossano fault zone; TAB, Transpressed Apulian Block; TFS, Tindari fault system; VA, volcanic arc. (For interpretation of the references to colour in this figure legend, the reader is referred to the web version of this article.)

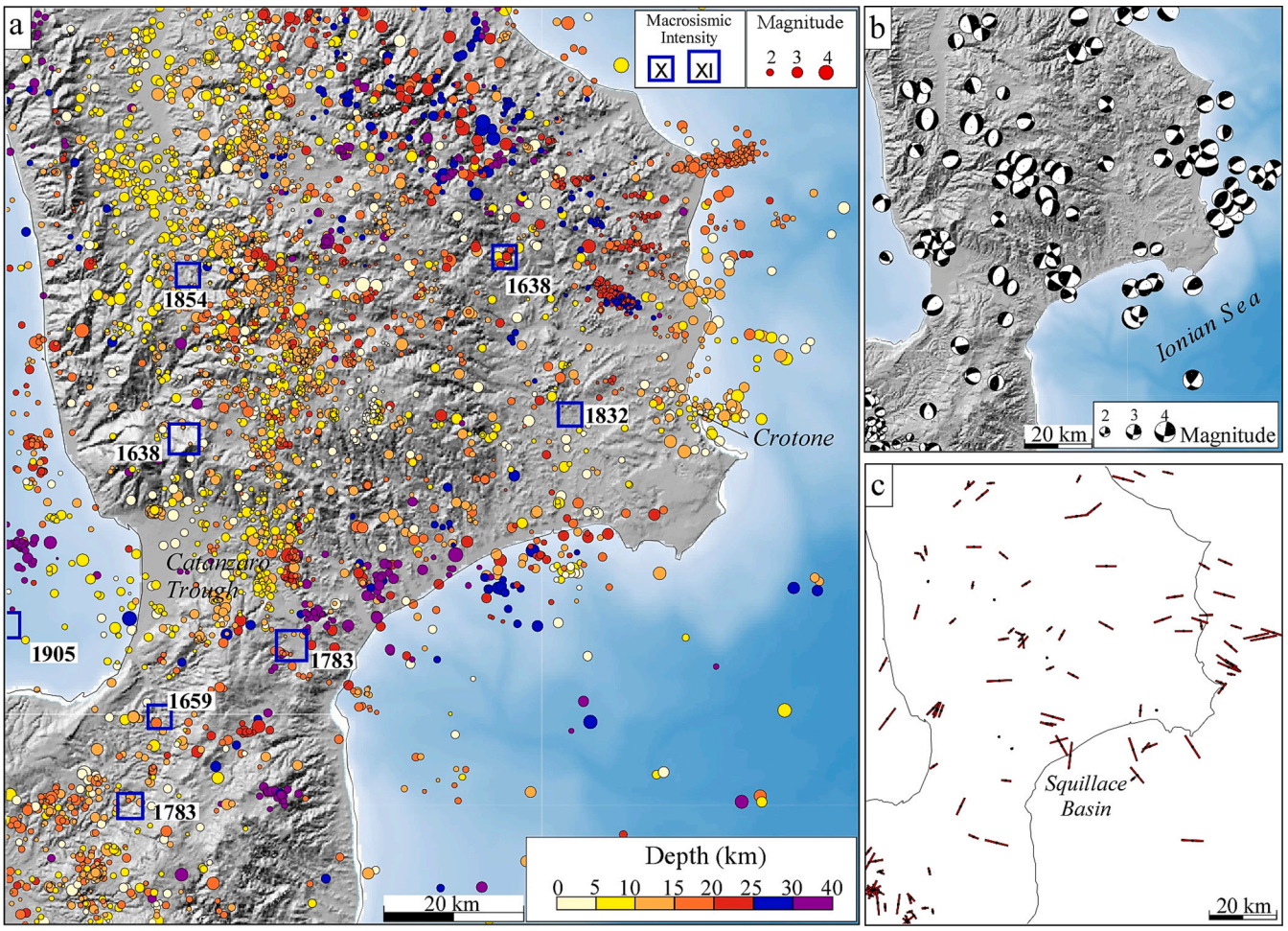


**Fig. 2.** a) Map of historical and instrumental seismicity with a maximum depth of 40 km, recorded since 1985 up-to-date. b) Focal mechanism solutions (Scarfì et al., 2021) and c) P-axes distribution.

et al., 2018) and related crustal deformation expressed by a strike-slip zone (Brutto et al., 2016; Corradino et al., 2021; Pirrotta et al., 2021), 2) the Plio-Quaternary development of NW-SE to WNW-ESE-trending regional strike-slip fault system located in the northern Calabrian Arc and associated with its south-eastward migration (Monaco et al., 1998; Tansi et al., 2007; Van Dijk et al., 2000), and 3) deformation at local scale that controlled the Plio-Quaternary tectonic evolution of the Squillace Basin (Capozzi et al., 2012; Del Ben et al., 2008).

In this structural frame, the Calabrian region represents one of the Italian areas with the largest concentration of seismic moment release (Calò et al., 2012; Frepoli and Amato, 2000) and a high probability of large earthquakes (Rotondi, 2010). In particular, the area of the Catanzaro Trough and its western offshore, the Sant'Eufemia Gulf, was affected by historical seismic events with a magnitude M > 6.5. In the Ionian offshore, the distribution of instrumental seismicity shows scattered events with a maximum magnitude of 4.3.

During the last decade, several geological and geophysical studies were carried out in the Calabrian Arc and its offshore to identify the tectonic structures and their kinematic (Brutto et al., 2016; Capozzi et al., 2012; Corradino et al., 2020, 2021; Del Ben et al., 2008; Ferranti et al., 2014; Mattei et al., 2002; Monaco and Tortorici, 2000; Tansi et al., 2007; Van Dijk et al., 2000; Zecchin et al., 2020) as well the seismic potential of this area (e.g. Neri et al., 2020; Presti et al., 2013; Scarfì et al., 2018). However, most studies concentrated on the deep seismicity associated with intraslab events. Therefore the relationships between recent deformation and shallow seismicity (< 15 km) need to be investigated.

This study aims to define the structural pattern of the Squillace Basin by analysing seismic reflection profiles at different resolution/penetration, calibrated with well-log, multibeam bathymetric data and seismicity distribution map. A multiscale approach was used to distinguish different orders of faults (minor and major structures), characterise their geometry and obtain geological constraints to identify the structures potentially associated with large earthquakes that struck the eastern Calabrian region (Rovida et al., 2021).

The data and interpretation we present, integrated with regional knowledge, give new insights into the active tectonics of the central Calabrian Arc.

## 2. Geological and seismological setting

### 2.1. Tectonics of the Calabrian Arc

The Calabrian Arc is an arc-shaped segment of the Apennine-Maghrebian fold-and-thrust belt (Fig. 1a-c) that connects the NW-trending Apennine chain to the *E*-trending Sicilian Maghrebides in the context of the Africa-Europe convergence (Patacca et al., 2004). Its shape was associated with the diachronous collision of the Apennine belt with the Apulian foreland to the north and the Hyblean foreland to the south (Van Dijk et al., 2000) and the residual subduction and roll-back of the Ionian slab that, in turn, caused rapid SE migration of the Calabrian Arc (Faccenna et al., 2005) and its fragmentation in NW-SE elongated blocks (Knott and Turco, 1991; Van Dijk, 1991; Van Dijk and Scheepers, 1995). The latter moved independently through regional strike-slip fault

systems: Pollino and Sangineto line to the north and its offshore prolongation (Ferranti et al., 2009, 2014; De Ritis et al., 2019), Lamezia-Catanzaro line in the centre (Pirrotta et al., 2021; Tansi et al., 2007) and its offshore prolongation (Corradino et al., 2021), and Tindari line in the northeastern Sicily (Barreca et al., 2019; Cultrera et al., 2017; Scarfì et al., 2018). Regional extensional/transtensional faults developed along the western sectors of the Calabrian Arc (Monaco and Tortorici, 2000; Spina et al., 2011), coeval to the Quaternary uplift with a rate of ~1 mm/year (Ferranti et al., 2009; Molin et al., 2002; Pepe et al., 2014).

The Northern Calabrian Arc (NCA) and its offshore consists of the Sila Massif, Coastal Chain, and several sedimentary basins (Fig. 1b), located along its western (Crati, Paola and Amantea basins) and eastern margin (Sibari Plain and Crotone basin) and to the south (Sant'Eufemia, Catanzaro and Squillace basin).

Regional NW-SE strike-slip fault systems (ACFZ, PSFZ and SRFZ, Fig. 1b) cut the central-eastern sector of the NCA (Monaco et al., 1998; Tansi et al., 2007; Van Dijk et al., 2000), suggesting a NW-SE trending left-lateral crustal shear zone. Strike-slip fault systems and associated tectonic structures also formed a) in the hinge zone of the Paola Anticline (PA, Fig. 1b) from the Late Pliocene to Early Pleistocene times (Corradino et al., 2020), b) in the Amendolara Ridge during the Middle-Late Pleistocene (AR, Fig. 1b, Del Ben et al., 2008, Ferranti et al., 2014), c) in the Calabrian accretionary wedge during the late Pliocene (TBA, Fig. 1b, Volpi et al., 2017), and d) in the Sant'Eufemia Gulf since the Early Pliocene (Brutto et al., 2016; Corradino et al., 2021).

The tectonic evolution of the other basins developed in the NCA and its offshore since the Middle Miocene was reconstructed by a lot of authors and explained with contrasting models: 1) extensional tectonics was proposed for the formation of Crati and Amantea basins since the Serravallian (Brozzetti et al., 2017; Mattei et al., 2002); 2) NW-SE trending left lateral regional crustal shear zone was considered to have the main control in the developing of Crati and Sibari basins since the Early Pleistocene (Spina et al., 2011; Tansi et al., 2007); 3) extensional tectonics, interrupted by compressional or transpressional events, was considered responsible for the evolution of the Paola Basin (Milia et al., 2009), Crati Basin (Knott and Turco, 1991), Crotone Basin (Consolaro et al., 2013; Massari et al., 2010; Van Dijk, 1991; Zecchin et al., 2020), Sant'Eufemia Gulf (Brutto et al., 2016; Corradino et al., 2021) and Squillace Basin (Capozzi et al., 2012); 4) shortening was supposed to control the formation of the ~5 km deep Paola syncline (Pepe et al., 2010; Corradino et al., 2020) and piggyback or perched basins in the frame of the eastward migration of the Apennine fold-and-thrust belt (Monaco et al., 1996).

We refer to the age of the above-mentioned tectonic events in the 2022 version of the International Chronostratigraphic Chart (ICS, Cohen et al., 2013; updated). The change regards the Gelasian, included in the Pliocene in older versions of ICS and now belonging to the Pleistocene as the lowest Stage/Age.

### 2.2. Seismotectonic framework

Central Calabria has been affected by strong earthquakes generated by crustal faults (DISS Working Group, 2018) in historical times (Fig. 2). Among these, the March 1783 event with Mw of 7 and Io of 11 occurred in the area of the Catanzaro Trough, the 1905 event with Mw of 7.0 affected the Sant'Eufemia Gulf, and the March 1832 earthquake with M of 6.6 occurred in the Crotone area (Rovida et al., 2021).

The analysis of GPS data (Devoti et al., 2017) and focal mechanisms (Scarfì et al., 2021; Totaro et al., 2016) indicates that western Calabria is characterised by an NW-SE oriented extensional tectonic regime associated with large magnitude earthquakes (e.g., Galli and Peronace, 2015). In contrast, the Ionian margin of the Calabria region is affected by strike-slip tectonics associated with the oblique plate convergence (Totaro et al., 2016) and by active compressional structures related to the migration of the Calabrian accretionary wedge (e.g., Gutscher et al., 2017; Polonia et al., 2011).

### 2.3. Study area: Squillace Basin

The Squillace Basin is located in the Ionian offshore of the Calabrian Arc (Fig. 1b). The southern and northern boundaries of the Squillace Basin are the Punta Stilo swell (Mangano et al., 2022) and the onshore Crotone basin, respectively. A complex canyons system connects the narrow shelf with the deep basin. Also, its slope is characterised by recent seabed morphologies such as slides and slumps (Morelli et al., 2011). To the north of the basin, a mega landslide (at least 500 $km^2$, orange dotted line in Fig. 1b) moves towards the Ionian Sea through a Messinian salt layer (Minelli et al., 2013; Zecchin et al., 2018).

According to Del Ben et al. (2008), the evolution of the Squillace Basin was controlled by a generalised transtensional tectonic regime. The prominent feature is the west-east trending trough located in its central sector. It is filled by Middle-Upper Miocene sequences, covered by about 2.5 km thick Plio-Quaternary deposits. The steep depression is associated with a W-E trending, left lateral transtensional fault developed during the Pliocene, whose western extension is considered the WNW-ESE transtensional Lamezia-Catanzaro system (Del Ben et al., 2008). The latter bounds to the north the Catanzaro trough and separates the northern and southern Calabrian Arc (Guarnieri, 2006; Pirrotta et al., 2021; Tansi et al., 2007; Van Dijk et al., 2000). Other authors documented transtensional tectonics from the Messinian to Middle Pliocene that caused the formation of a roughly NW-SE-oriented narrow basin (e.g., Capozzi et al., 2012). This tectonic event was followed by a Late Pliocene – Early Pleistocene compressional event, which led to the development of a thrust zone in the northern Crotone swell and recent extensional tectonics that affected the sedimentary infill of the Squillace Basin.

## 3. Seismological data and analysis

The seismic activity of the Calabrian Arc has been instrumentally recorded since the early 1980s. In order to visualise possible cluster alignments and reconstruct the geometry of the faults in the studied area, the seismic events were selected from the available database (https://istituto.ingv.it/it/risorse-e-servizi/archivi-e-banche-dati.html) in the period 1981–2022 and were relocated by using the tomoDDPS code (Zhang et al., 2009). This algorithm has the advantage of improving hypocentre location through a combination of absolute and differential arrival-time readings between couples of closed-spaced earthquakes and by using a 3D velocity model – here we adopted the velocity model of Scarfì et al. (2018), suitable for the Calabrian area.

Event distribution highlights that most earthquakes are located in the Calabrian onshore. Their hypocentral depth is mainly in the range of 5–20 km in the western sector. Moving towards the Ionian zone, i.e. north of Crotone and into the Catanzaro Trough, foci of earthquakes show greater depths, along with some NW-SE hypocentral alignments (Fig. 2a).

Focusing on the Squillace Basin, about 300 earthquakes occurred in the last 40 years along the coastal area and offshore, with magnitudes mainly in the range of 1.0–3.0 and a maximum of 4.3 (Fig. 2a). Most of the events concentrate in the northern sector, and their hypocentral depth varies between shallow to about 30 km (Fig. 2a). Focal mechanisms of earthquakes located in the basin and along the central-western coast, some within 10 km of depth, indicate mainly strike-slip or transpressive movements (Fig. 2b), with P-axes oriented about NW-SE to NNE-SSW (Fig. 2c).

## 4. Marine data and methods

Multibeam bathymetry and seismic reflection data (MCS Airgun and Chirp sonar) are part of the seismic dataset acquired in two oceanographic cruises on board the N/O Explora of the Osservatorio Geofisico Sperimentale (OGS) by the University of Trieste (Italy). In particular, the data set was acquired in the frame of the "Morphology and Evolution of

the Submarine Canyons in the Ionian Margin of Calabria" Project of the University of Trieste, Italy (MESC05; Morelli et al., 2011) and "MAGIC" campaign funded by the Italian Civil Protection in 2005 and 2009, respectively.

### 4.1. Multibeam bathymetry

Swath bathymetric data were collected using multibeam systems at different frequencies. The Reason Seabat 8111 (100 kHz) and the Reson SeaBat 8150 (12 kHz) were used in shallow and deep water, respectively. Data processing included: a) patch test on calibration lines, b) tide corrections, c) statistical and geometrical filters to remove coherent and incoherent noise, and d) manual removal of spikes. Processed data were gridded, generating DEMs with cell sizes varying from 10 m in shallow water (<100 m) to 50 m in deep water (>500 m). The bathymorphological map was projected in UTM 33 N—Datum WGS84.

### 4.2. Seismic reflection data acquisition and processing

Over 90 km of multichannel high-penetration reflection (Airgun) seismic data and ultra-high resolution reflection (Chirp) seismic data (orange and white lines, Fig. 2a) were recorded in the Squillace Basin.

Airgun profiles are primarily oriented in the NNE–SSW direction, with crossline seismic profiles acquired along the WNW–ESE direction. A 48-channel streamer with an active length of 600 m recorded the signals generated by two GI-Gun of 2 × 355 cubic in of total volume. A DGPS system controlled the navigation positioning. The processing sequence included the following operations: geometry assignment by 2D CDP profiles binning, DC removal, signature deconvolution, F-K filter, trace stacking, static corrections, velocity analysis, multiple attenuations, post-stack Kirchhoff time migration, time-variant bandpass filtering and automatic gain control removal to restore the True Amplitude. Signal penetration exceeds 4 s two-way time (t.w.t).

Ultra-high resolution seismic-reflection data were recorded using the Chirp II (Benthos©inc) sub-bottom profiler, which operates with 16 transducers in a wide frequency band (2–7 kHz), and a chirp pulse of 20–30 ms. The shot interval was 0.5 s. Acquired profiles run mainly along the NE-SW direction and are tied by lines recorded mainly in the NW-SE direction (see Fig. 2a for location). A DGPS system controlled the navigation positioning. Data were processed running the following mathematical operators: a) true amplitude recovery using a $T^2$ spherical divergence correction, b) time-variant gain to boost amplitudes of deeper arrivals and c) mutes to eliminate the signal noise on the water column. Signal penetration exceeded 80 ms t.w.t. in the deeper sector of the basin. Vertical resolution is up to 5 cm beneath the seafloor. Seismo- and sequence stratigraphy-based analysis facilitated the reconstruction of the depositional architecture of seismic-stratigraphic units. Seismic units were calibrated using well-log data (Fig. 2b).

An additional grid of MCS profiles from Vi.DE.PI database (yellow lines, Fig. 2a) was used for this study (https://www.videpi.com/videpi/sismica/sismica.asp). The MCS sections were converted from raster to SEG-Y format using the GeoSuite AllWorks software. The geodetic reference system is the WGS84 with a UTM 33 N projection.

## 5. Results

### 5.1. Morpho-bathymetry of the Squillace Basin

The Squillace Basin is a portion of the Ionian continental margin of about 6000 $km^2$, where the continental shelf extends from a few hundred meters to 8 km (Fig. 4), whether the slope is wide up to 50 km and steep from 2° up to 8°.

The most prominent bathymetric feature in this area is the Squillace canyon, a 40 km-wide and >50 km-long shelf incised structure (Fig. 4). The Squillace canyon consists of a complex system of canals and three main branches (B1–3, Fig. 4). The latter are characterised by composite heads (CH, Fig. 4) that deeply intersect the shelf from the northwest (in front of Catanzaro) to southwest. The three composite heads link towards the slope with well-carved erosive valleys. Their thalwegs show variable trends with sinuous and meandering sections (CH2 and CH3) or a straight section interrupted by a sharp deviation (CH1). Despite these complex trends, it is possible to recognise a general counterclockwise rotation of the directions of the three main branches from NW-SE (upper reach of B1) to WNW-ESE (B3), moving from northwest to southwest along the basin.

A second shelf incised canyon, named Botricello, develops in the northern part of the basin (Fig. 4). It is smaller (8 km wide and about 40 km long) and characterised by two branches <15 km long. The canyon's heads have a landward retrogressive erosion character and are responsible for the repeated turbidity currents occurring along the canyon (Ceramicola et al., 2014; Loher et al., 2018).

Several WNW-ESE to NW-SE morphological highs up to 4 km long and 2 km wide dissect the slope of the basin (Fig. 4). They occur both adjacent to the main canyon body and across the headwalls. In particular, two morphological highs, located between branches B1 and B2 of the Squillace canyon, are delimited by steep and rectilinear scarps and are dissected by minor NW-SE escarpments.

WNW-ESE elongated scarps limit wide terraces within the slope north to the Punta Stilo swell (dotted lines, Fig. 4).

### 5.2. Seismo-stratigraphic characterisation and interpretation

Two seismo-stratigraphic units, named from bottom to top as unit MD and PQ, were identified based on their bounding unconformities and seismic characters (e.g., amplitude, lateral continuity, and frequency of internal reflectors).

Unit MD is characterised by subparallel, locally discontinuous, medium frequency, and medium-to-high amplitude reflectors. Its boundaries at the top and bottom correspond to high-amplitude reflectors. The reflectors are sub-horizontal in the southern and northern sectors of the basin (CDPs 0–400, Fig. 5a; CDPs 0–100, 700–900, Fig. 5b), whereas they are inclined in the central sector (CDPs 500–1100, Fig. 5a; CDPs 200–700, Fig. 5b). The upper limit was associated with the top of evaporites deposited during the late Messinian salinity crisis or an erosional unconformity formed during the late Messinian sea level fall (Just et al., 2011 and references therein). We correlate unit MD with the Upper Miocene deposits based on the seismic signature and well-log data.

Unit PQ overlay the M horizon and is characterised by continuous, high-to-medium frequency and medium-to-high amplitude reflectors. Based on its seismo-stratigraphic position and well-log data, we correlate unit PQ with the Plio-Quaternary sedimentary succession widespread in the Tyrrhenian Sea. In the central sector of the basin, we have recognised an unconformity surface (US1) that separates the unit PQ into two subunits, labelled PPL and CR, from bottom to top (CDPs 600–1100, Fig. 5a). Well-seismic calibration indicates that the US1 formed during the Early Pleistocene (Calabrian). In the other sector of the basin, the US1 becomes a conformity surface.

Subunit PPL consists of a series of subparallel reflectors with an aggradational internal geometry. The strata paraconformably overlay the M horizon and locally show onlap terminations onto the M horizon (around CDP 12900, Fig. 5a).

Subunit CR is marked by layered reflectors with onlap geometry onto the unconformity US1 in the central sector of the basin (Fig. 5a). Here, the strata are inclined with a wedge geometry and become subhorizontal upwards. In the southern and northern sectors of the basin, strata are generally characterised by a sub-horizontal horizontal geometry. Subunit CR is bounded upwards by the seafloor.

Within the subunit CR, an unconformity surface, named US2, was recognised in the central sector of the basin (Fig. 5b). The overlaying deposits show onlap termination onto the surface.

In the northern sector of the basin, the two subunits of PQ are not

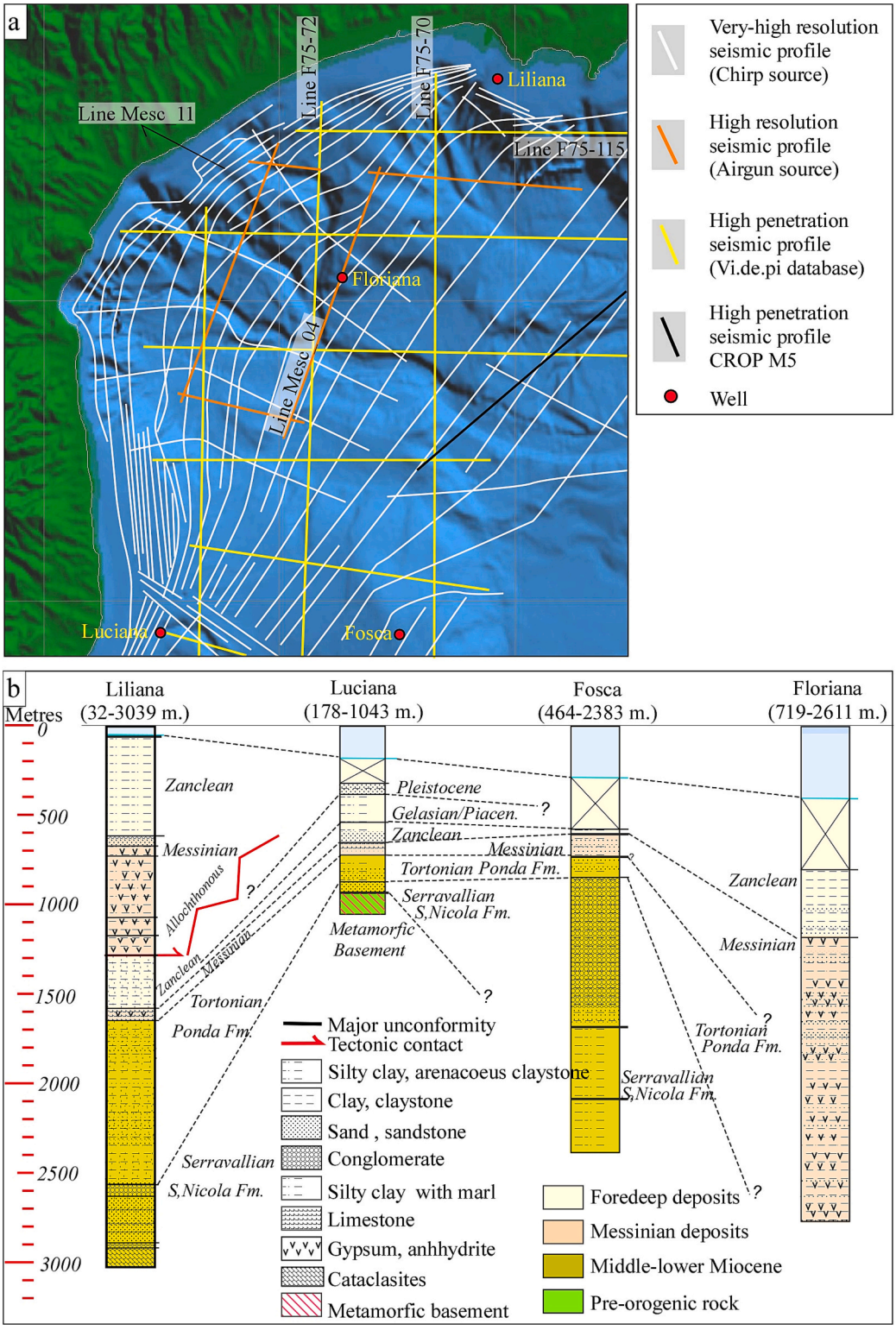


**Fig. 3.** (a) Grid of seismic profiles and location of wells used for this study. See Fig. 1b for the location of the map. (b) Stratigraphic correlation among selected wells in the Squillace Basin.

detectable due to the Crotone Megaslide (Minelli et al., 2013). The slide's base lies roughly at a depth of 1.5 s and corresponds with an erosional surface that cut the post-Messinian deposits (blue reflector, Fig. 5c).

### 5.3. Fault systems of the Squillace Basin

Normal faults offset the Unit MD with opposite dipping towards the south and north, bounding horst and half-graben structures (Figs. 5a, b and c; 6a and b). Upper Miocene deposits seal them, except for the northern sector of the basin, where the faults cut the M horizon (Fig. 5c).

In the central sector of the basin, a major fault cut the deposits of Unit

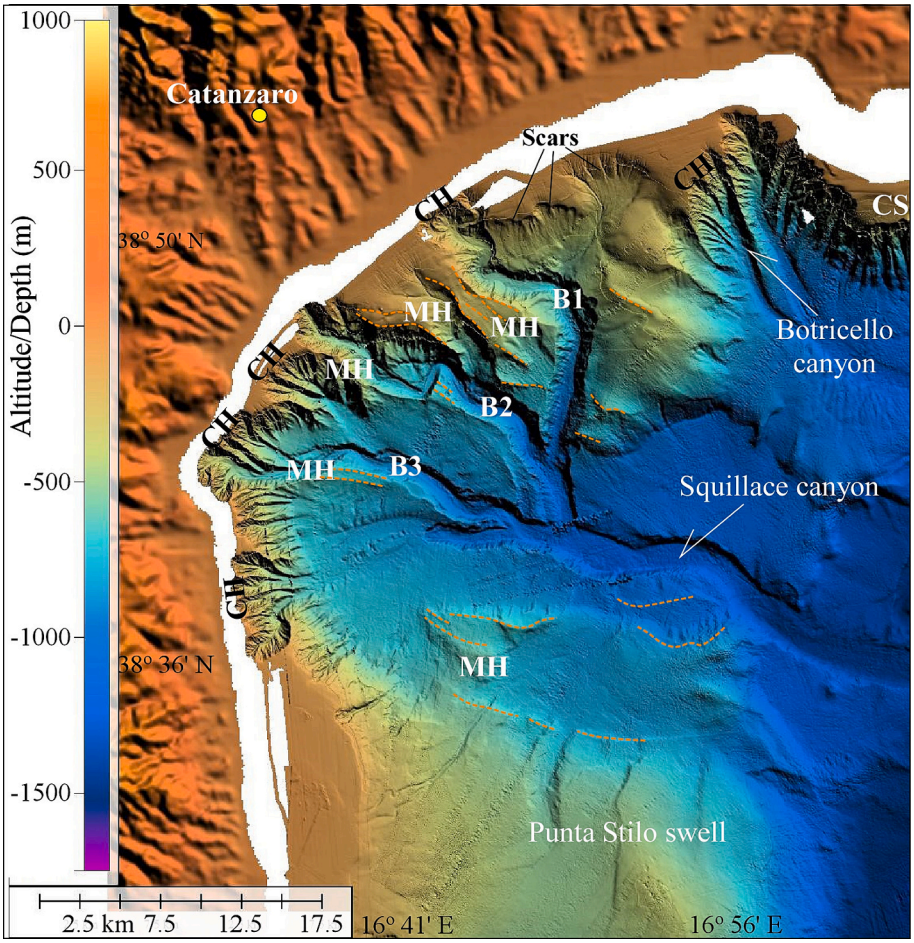


**Fig. 4.** Morpho-bathymetric map of the Squillace Basin. Orange dotted lines indicate scarps. B1–3, Main branches of the Squillace canyon; CH, canyon heads; CR, Crotone swell; MH, morphological high.

MD and the lower part of Unit PPL with a sub-vertical fault plane (around CDP 800, Fig. 5a; around CDP 400, Fig. 5b). The thickness of Unit MD on both sides of the fault plane is different. The geometry of the fault and the thickness mismatch suggest the strike-slip kinematics of this structure. In plan view, this fault develops with a roughly WNW-ESE orientation (Fig. 6b).

Some normal faults show a younger activity, reaching the deposit of the subunit CR (CDPs 500–600-1050, Fig. 5a; CDPs 150–700, Fig. 5b; Fig. 5c). Thickening deposits were recognised in the hanging wall of the faults, and the upper part of the fault planes shows a reverse kinematic (e.g. CDPs 600–800, Fig. 5a; around CDP 200, Fig. 5b; around CDP 100, Fig. 5c). Based on these features, the younger faulting is interpreted as the result of positive inversion process, associated with a transpressional tectonic phase. The inversion is partial (sensu Williams et al., 1989) because the faults maintain a normal displacement in depth (e.g. around CDP 1050, Fig. 5a). The transpressional reactivation of main faults dipping towards the centre of the basin led to uplift and bending of the previous basin fill (Fig. 5a and b). The shortening, related to the transpressional faults, formed a ~ 1.2 km-deep *E*-W trending depression located in the central sector of the basin. Other minor compressional/transpressional faults (around CDP 1300, Fig. 5a) and splays formed close to the main structures (around CDP 550, Fig. 5a). In the central sector of the basin, the depression is filled by deposits of the subunit CR that show onlap termination onto the top of the subunit PPL (Fig. 5a). The lower part of the subunit CR is characterised by growth strata, suggesting a deposition during the transpressional reactivation of the main faults. Considering that the bottom of this subunit is aged at ~1.8 Ma (US1, Fig. 5a), it is possible to date the beginning of the transpressional deformation at the Early Pleistocene (Calabrian). Thus, the unconformity US1 has a tectonic origin.

In the other sectors of the basin, subunit CR was also involved in shortening (CDPs 600–700, Fig. 5b; around CDP 100 and 300, Fig. 5c). The transpressional structures displaced the lower part of subunit CR, folded its upper part and controlled the formation of unconformity surfaces within the subunit CR. The deep (>3 km) transpressional faults show NNW-SSE to WNW-ESE orientation in plain view and are associated with ridges bounded by canyons in the northern and western sectors of the basin (Fig. 6c).

NW-SE to WNW-ESE trending, high-angle normal faults offset the subunit CR (Fig. 7a and b). Some of these faults cut older units, reaching a maximum depth generally <2 km (using 1800 m/s for time-to-depth conversion). Some of these faults propagate upwards, reaching the seafloor (Fig. 7b). The fault throw measured at the seafloor varies from a few meters to a few dozen meters, and, consequently, they have a mild morphological expression (Fig. 6c). An exception is in the southern area of the basin, where a series of north-dipping normal faults correspond to WNW-ESE elongated scarps bounding wide terraces within the slope.

## 6. Discussion

### 6.1. From deep to shallow: tectonic interpretation of the Squillace Basin

The multiscale approach, coupled with the morpho-bathymetric map analysis, allowed us to define three steps in the structural evolution of the Squillace Basin from the Late Miocene to Recent times.

The first event was characterised by a late Miocene extensional

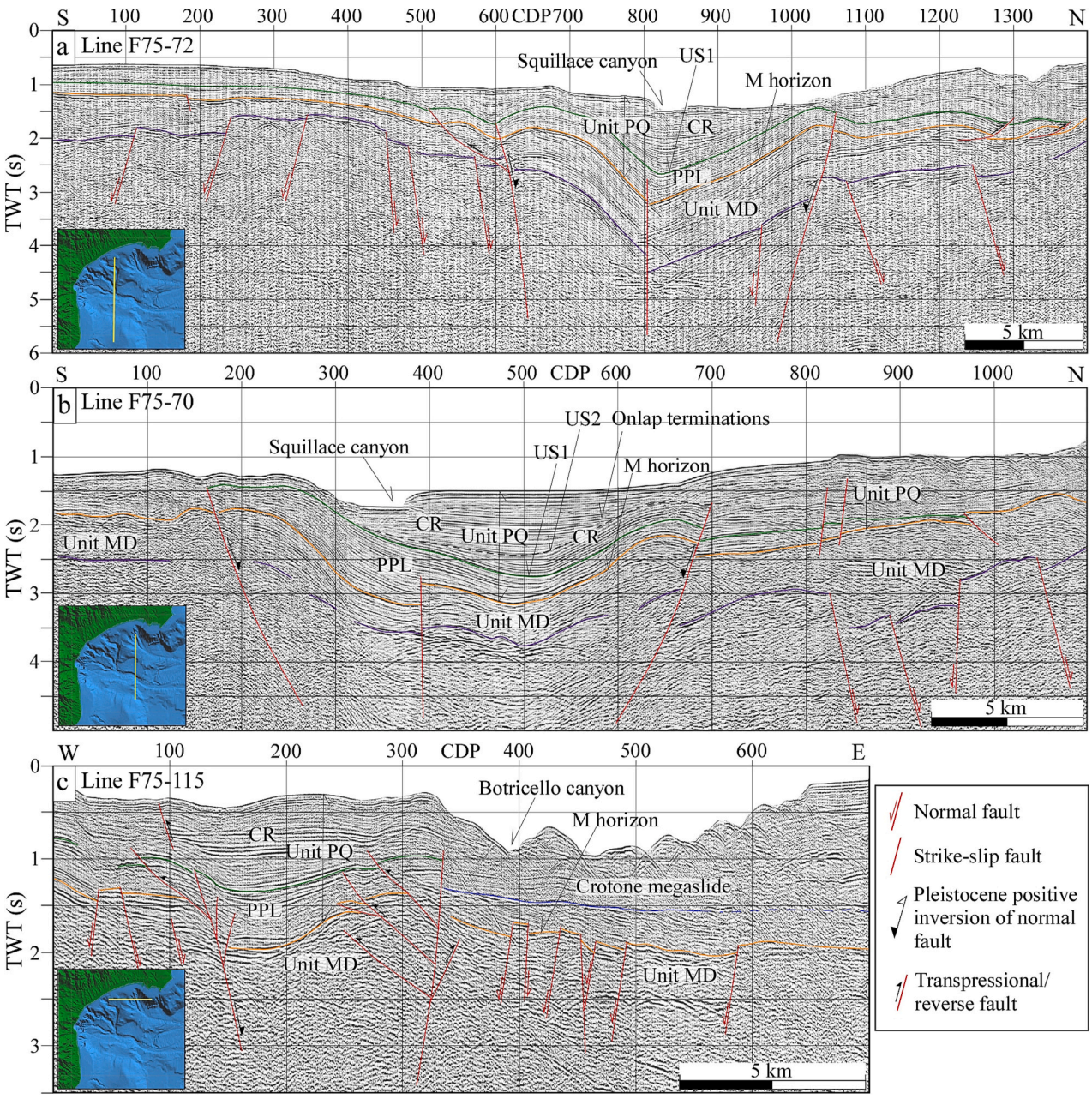


**Fig. 5.** (a), (b) and (c) High penetration seismic profiles "Line F-75-72", "Line F-75-70" and "Line F-75-115", respectively, and their interpretation. Insets show the location of the profiles.

deformation that led to the formation of a series of roughly WNW-ESE-oriented horst and half-graben structures. Our results agree with previous findings concerning the Messinian transtensional structures recognised by Capozzi et al. (2012). A late Miocene extensional event was also documented in the Crotone Basin (Massari and Prosser, 2013), Amantea Basin (Mattei et al., 2002) and Sant'Eufemia Gulf (Brutto et al., 2016; Corradino et al., 2021). The extensional tectonics in the study area and surroundings is supposed to be related to the intense stretching of the continental crust that occurred in the central Mediterranean in response to the opening of the Tyrrhenian Basin since late Tortonian (Pepe et al., 2000; Spadini et al., 1995).

During the Pliocene, deformation concentrated in the central and northern sectors of the Squillace Basin (Fig. 6b). In the central sector, evidence of strike-slip deformation comes from the thickness mismatch of the Unit MD on both sides of the fault (CDPs 700–900, Fig. 5a; CDPs 300–500, Fig. 5b). Based on the constant wide of the horsts and grabens observed in seismic profiles (Fig. 5a and b), we cannot exclude that the strike-slip reactivation involves one of the normal faults formed during the late Miocene extensional event. The end of fault activity was probably in the Early Pliocene, as suggested by deposits of the subunit PPL that are offset in the lower part only (CDP 800, Fig. 5a; CDP 400, Fig. 5b). The strike-slip structure can be linked to a deeply rooted NW-SE oriented fault interpreted in the Line CROP M5 (black line, Fig. 3a) by Capozzi et al. (2012), forming releasing bends. In map view, the strike-slip fault is observed to step to the right suggesting that its kinematics is dextral (Fig. 6b). Both the right-lateral kinematics of the fault and its age agree with the Pliocene – Early Pleistocene right-lateral transpressional tectonic event occurred in the Sant'Eufemia Gulf.

In the northern sector of the Squillace Basin, the Pliocene tectonics caused the formation of a series of normal to transtensional faults that offset the upper Miocene deposits (Figs. 5c, 6b).

Since the Early Pleistocene (Calabrian), strike-slipe tectonics affected

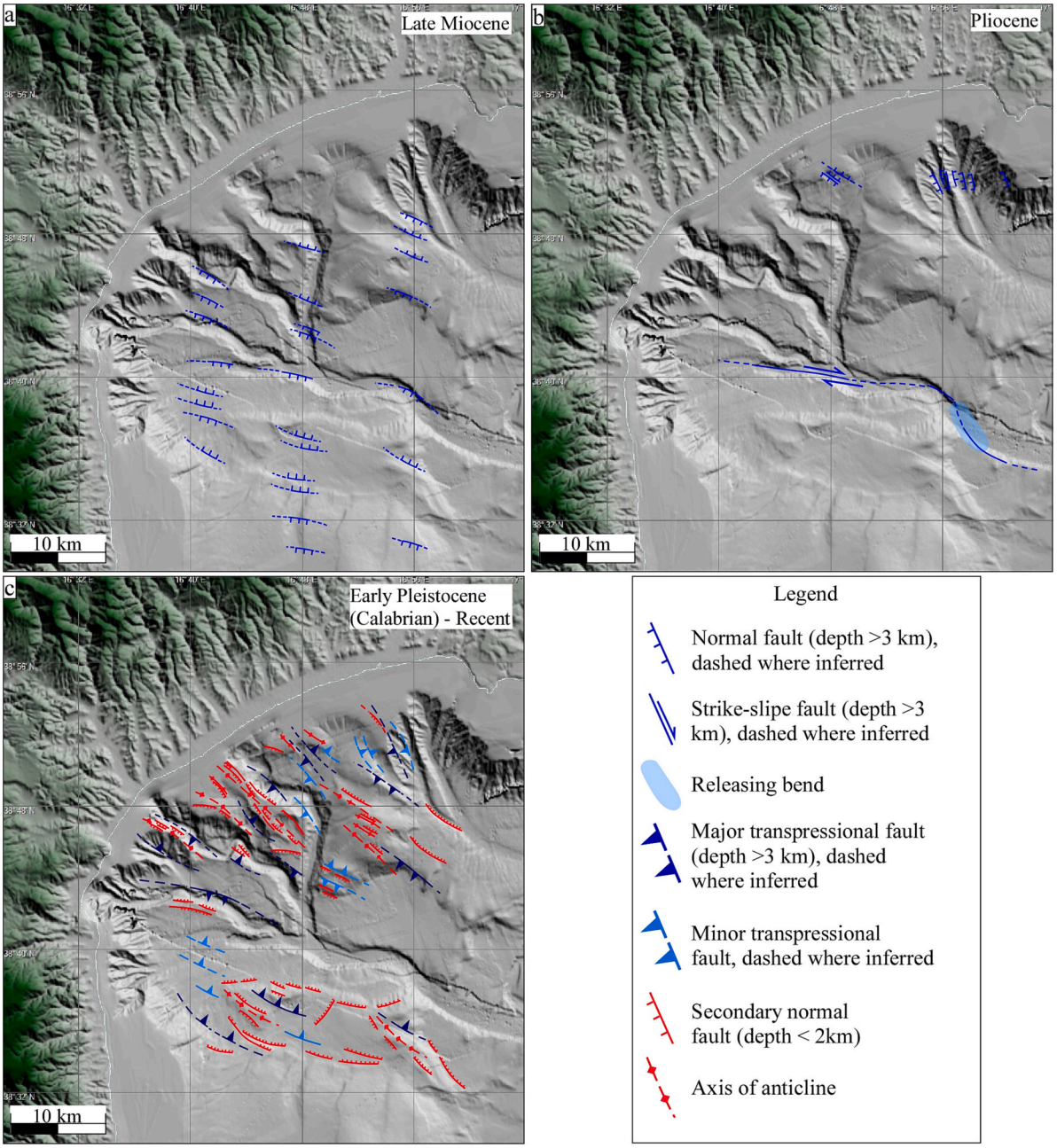


**Fig. 6.** Structural maps of the Squillace Basin showing fault systems active during (a) the Late Miocene, (b) the Pliocene and (c) the Quaternary. Quaternary secondary normal faults are mostly related to deformation occurring in the anticline extrados of deep transpressional faults.

a large part of the Squillace Basin (Fig. 6c), causing the positive inversion of deep (> 3 km) extensional faults inherited from the previous events (around CDP 600 and 1050, Fig. 5a; around CDP 150 and 700, Fig. 5b) and the formation of new reverse faults (around CDP 1300, Fig. 5a; around CDP 900; Fig. 5b).

The reactivation of deep faults was diachronous, as suggested by the unconformity surface S2 recognised within the subunit CR (Fig. 5b). This surface terminates onto a limb of an anticline associated with the development of the transpresional fault in the southern sector of the basin (around CDP 300, Fig. 5b), indicating that the structure developed before the formation of the surface S2. Conversely, the same surface is involved in the deformation of an anticline in the central part of the basin (CDPs 500–700, Fig. 5b). These geometries suggest the transpressional event in the centre of the basin occurred later than in the southern part. Also, the onlap terminations of the deposits of the subunit CR onto the anticline limb in the central sector (around CDP 600, Fig. 5b) indicate that the transpressional fault and related anticline are no longer active. Conversely, the transpressional fault, which affects the southern sector of the basin (around CDP 200, Fig. 5b), deforms the seafloor suggesting its current activity.

In the northern and western sectors of the basin, transpressional and reverse faults are NW-SE oriented, cut deposits of the subunit CR and propagate upwards, folding the shallower deposits (e.g. Figs. 5c, 7a). To the south, the transpressional faults show a WNW-ESE orientation along the Stilo Swell margin. The transpressional structures have a morphological expression at the seafloor, forming ridges bounded by canyons. North of the Squillace Basin, the Crotone Basin (Fig. 1b) was also affected by compressional deformational during the middle Pleistocene, with a NE-SW oriented vector of maximum shortening (Zecchin et al., 2020). This direction is compatible with the orientation of the

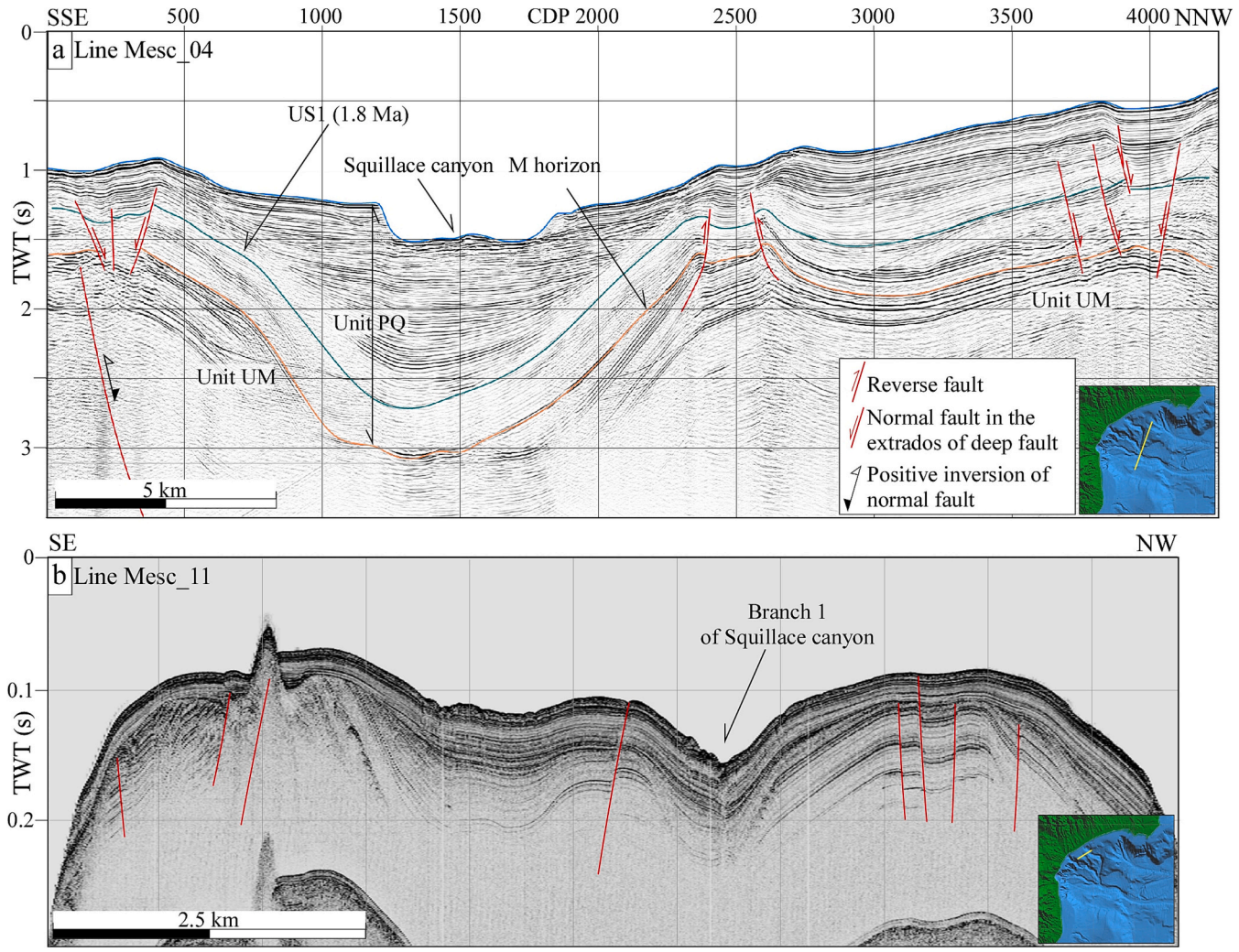


**Fig. 7.** (a) and (b) High and very-high resolution seismic profiles "Line Mesc_04" and "Line Mesc_11", respectively, and their interpretation. Insets show the location of the profiles.

transpressional structures developed in the Squillace Basin.

In correspondence with the deep transpressional faults, a series of high-angle normal faults offset the subunit CR (Fig. 7a). Some faults offset the seafloor and form morphological scarps (Figs. 4, 7b), thus suggesting that they were active during the Holocene. These shallow normal faults are NW-SE to WNW-ESE oriented, parallel to the elongated axis of the morpho-bathymetric ridges (Fig. 6c). Based on their depth and direction, we interpret these faults as secondary structures formed due to tensional stress in the extrados of anticlines associated with the deep transpressional faults. Thus, we propose that the transpressional structures and associated minor faults are active from the Calabrian to recent times. Conversely, Capozzi et al. (2012) interpret the formation of the recent normal faults as a consequence of an extensional regime that affected the study area during the Quaternary. Our interpretation also differs from the evolutionary model proposed by Del Ben et al. (2008), which consider a generalised transtensional tectonic regime as the cause for the formation and development of the Squillace Basin since the Pliocene.

The kinematics of the transpressional faults defined in the Squillace Basin fits with the roughly NW-SE oriented left-lateral crustal shear zones documented along the northern Calabrian Arc (ACFZ, PSFZ and SRFZ, Fig. 1b, Civile et al., 2022; Monaco et al., 1998; Tansi et al., 2007; Van Dijk, 1991; Van Dijk et al., 2000). Here, extensional faults are reactivated in a transpressional regime in the Late Pliocene and Middle Pleistocene, forming anticlinal structures and resulting in a complex set of thin- and thick-skinned back-thrusts (Van Dijk et al., 2000; Van Dijk and Scheepers, 1995). Therefore, we propose that the transpressional structures in the northwestern sector of the Squillace Basin are the offshore prolongation of the Albi-Cosenza fault zone (ACFZ, Fig. 1b).

The growth of ridges associated with the deep transpressional faults results in a shallower bathymetry in the northern and western sectors of the Squillace Basin. Here, a series of canyons trending towards SE and ESE developed parallel to the elongated axis of the ridges. Our data suggest that their formation can be related to the uplift of ridges, which induced a lowering of the base level.

### 6.2. *Seismotectonic implications*

Our data and interpretation allow recognising two fault systems in the Squillace Basin. In particular, the deepest (> 3 km), NW-SE to WNW-ESE trending, transpressional faults in the northern and western sectors of the basin (Fig. 6c) fit with the structures of the fault zones that dissect the northern Calabrian Arc (Fig. 1b). The presence of push-up and antiformal folds that deform the younger deposits (subunit CR) and form ridges on the seafloor suggests their recent activity. The second fault system includes minor shallow (< 2 km) high-angle normal faults developed at the culmination of anticlines related to the deep transpressional faults. Some of these faults form escarpments at the seafloor, suggesting they are active.

The instrumental seismicity at a depth <15 km highlights the

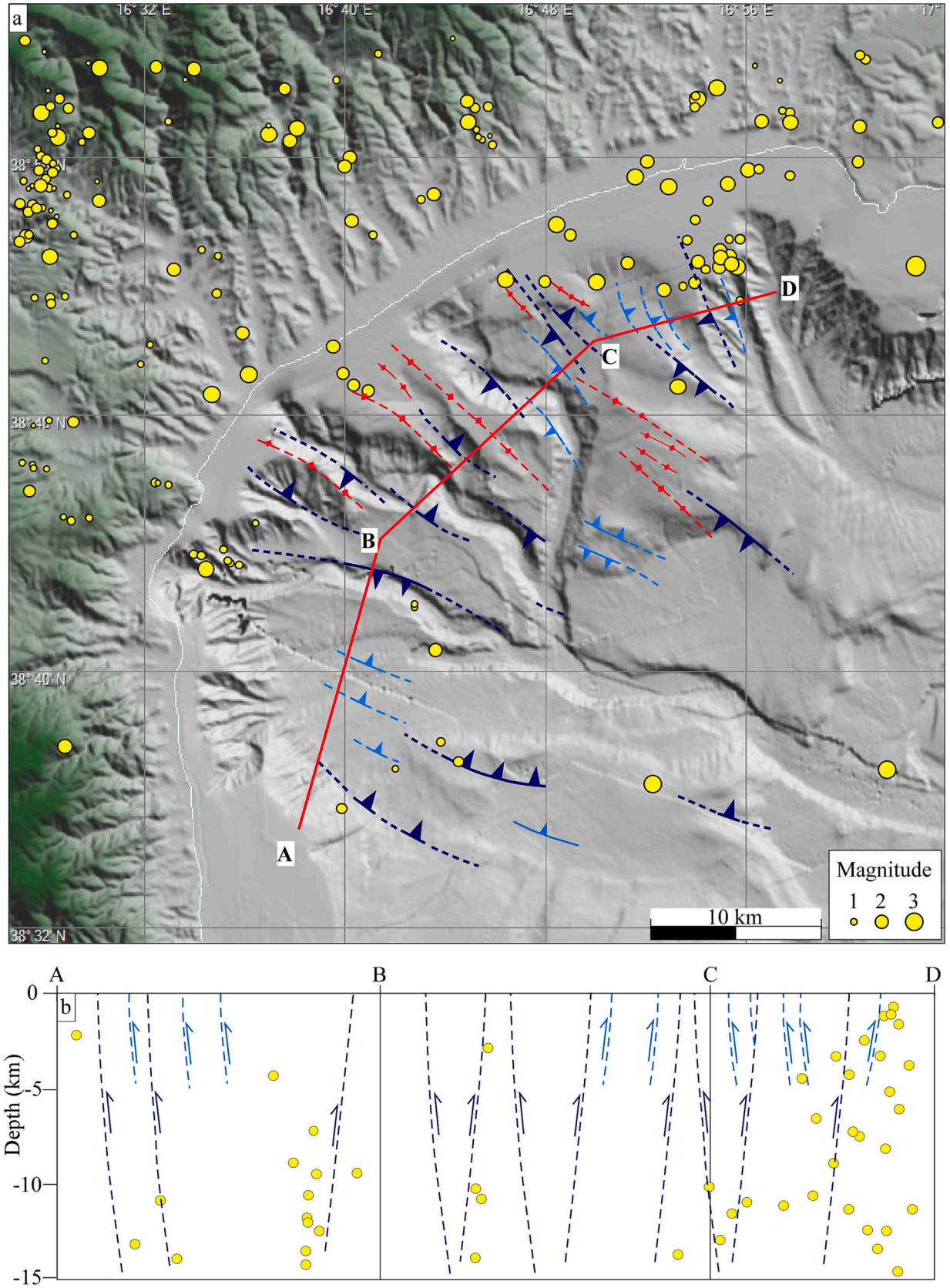


**Fig. 8.** (a) Structural map of the Squillace Basin showing the Quaternary fault systems and the distribution of seismicity in the range between 0 and 15 km. (b) Section ABCD showing the hypocenters of events located within 11 km on either side of the section. The dotted lines represent the faults intercepted by the section. The red line in panel a is the section trace. (For interpretation of the references to colour in this figure legend, the reader is referred to the web version of this article.)

occurrence of events in the northern, western and southern sectors of the Squillace Basin, located in the hanging wall of transpressional structures with a morphological expression on the seafloor (Fig. 8a and b).

Considering the distribution of the earthquakes that lies in correspondence with the transpressional structures, and the depth of hypocentres compatible with the depth of the transpressional faults, we suggest that deep transpressional structures are responsible for the major instrumental earthquakes that affected the Ionian offshore. Thus, seismo-stratigraphic and structural interpretation, supported by bathymetric and seismological data, suggest that the transpressional system is active and may be the source of future strong earthquakes and tsunamis.

The secondary structures (depth $< 2$ km) formed in response to tensional stress in the extrados of anticlines associated with the deep transpressional faults. Further, they offset incoherent Pliocene fine-grained and Quaternary coarser rocks even if some of these shallow faults cut the Messinian competent rocks (e.g. chalk at a depth of 1.6 km, Floriana well-log in Fig. 3b). Although these shallow secondary could be seismogenic, their length, depth, and the lithology of the deformed rocks suggest that they are inconsistent with hazardous seismicity.

## 7. Conclusions

A multiscale approach, based on the interpretation of seismic profiles with different resolution/ penetration, calibrated with well-logs, and integrated with bathymetric data and the distribution of instrumental earthquakes, allowed us to reconstruct the tectono-stratigraphic evolution of the Squillace Basin from the Late Miocene to Recent times. The results of this study also allowed identifying the active and seismogenic faults capable of producing large earthquakes and minor structures formed in response to local stresses in the extrados of anticlines. The main outcomes are summarised in the following.

The tectono-stratigraphic evolution of the Squillace Basin from the Late Miocene to Recent times consists of three steps. The first occurred during the Late Miocene and was characterised by extensional tectonics. During the Pliocene, strike-slip tectonics affected the central sector of the basin, while extensional to transtensional tectonics was dominant in its northern part. Since the Early Pleistocene, contractional and strike-slip movements caused the positive inversion of some deep ($> 3$ km) extensional faults and the formation of NW-SE to WNW-ESE transpressional/reverse faults and related anticlines.

The orientation of the Quaternary transpressional faults developed in the Squillace Basin is similar to that of the regional NW-SE fault systems (ACFZ, PSFZ and SRFZ, Fig. 1b) that cut the northern Calabrian Arc. Therefore, we propose that the Albi-Cosenza fault zone, which is the nearest to the study area, can be prolonged offshore, including the transpressional structures in the northwestern sector of the Squillace Basin.

Earthquakes with $M > 3$ and depth $<15$ km fall along the Quaternary transpressional faults, suggesting their recent activity and defining them as potential sources of large earthquakes.

Shallow ($<2$ km) normal faults developed at the anticline extrados associated with the deep transpressional faults. Some faults reach the seafloor suggesting that they are active faults. However, considering their length, shallow depth and the low competent rocks they cut, the shallow structures have a low seismogenic potential.

## Funding

This study has been partly funded by the project MUSE 4D-Overtime tectonic, dynamic and rheologic control on destructive multiple seismic events -Special Italian Faults and Earthquakes: From real 4-D cases to models, in the frame of PRIN 2017. The acquisition of the bathymetric data used in this research was funded by the OGS and Magic Project (Marine Geohazards along the Italian Coasts).

## Authorship

Marta Corradino: conceptualization, data curation, formal analysis, writing - original draft.
Danilo Morelli: formal analysis, writing - original draft.
Silvia Ceramicola: formal analysis, writing - original draft.
Luciano Scarfì: formal analysis, writing - original draft .
Graziella Barberi: formal analysis.
Carmelo Monaco: writing - review & editing.
Fabrizio Pepe: conceptualization, writing - review & editing.

## Declaration of Competing Interest

The authors declare the following financial interests/personal relationships which may be considered as potential competing interests:
Fabrizio Pepe reports financial support was provided by Government of Italy Ministry of Education University and Research.

## Data availability

Data will be made available on request.

## Acknowledgements

The authors would like to thank the crew of the oceanographic campaigns MESC and MAGIC 0409 onboard the n/r OGS Explora. The authors also thank Edy Forlin and Andrea Cova for processing the bathymetric data in the framework of the MAGIC Project. Ultra-high resolution seismic-reflection data processing and interpretation were performed within the GeoSuite AllWork software package. The PDS2000 software package process the swath bathymetric data.

The authors would like to thank the editor Ramon Carbonell, the reviwer Stéphane Dominguez and an anonimuos reviewer for their critical reading and useful comments that allowed us to improve the manuscript.

## References

Barreca, G., Scarfì, L., Gross, F., Monaco, C., De Guidi, G., 2019. Fault pattern and seismotectonic potential at the south-western edge of the Ionian Subduction system (southern Italy): New field and geophysical constraints. Tectonophysics 761, 31–45.
Brozzetti, F., Cirillo, D., Liberi, F., Piluso, E., Faraca, E., De Nardis, R., Lavecchia, G., 2017. Structural style of Quaternary extension in the Crati Valley (Calabrian Arc): evidence in support of an east-dipping detachment fault. Ital. J. Geosci. 136 (3), 434–453.
Brutto, F., Muto, F., Loreto, M.F., De Paola, N., Tripodi, V., Critelli, S., Facchin, L., 2016. The Neogene-Quaternary geodynamic evolution of the central Calabrian Arc: a case study from the western Catanzaro Trough basin. J. Geodyn. 102, 95–114.
Calò, M., Dorbath, C., Luzio, D., Rotolo, S.G., D'anna, G., 2012. Seismic velocity structures of southern Italy from tomographic imaging of the Ionian slab and petrological inferences. Geophys. J. Int. 191 (2), 751–764.
Capozzi, R., Artoni, A., Torelli, L., Lorenzini, S., Oppo, D., Mussoni, P., Polonia, A., 2012. Neogene to Quaternary tectonics and mud diapirism in the Gulf of Squillace (Crotone-Spartivento Basin, Calabrian Arc, Italy). Mar. Pet. Geol. 35 (1), 219–234. https://doi.org/10.1016/j.marpetgeo.2012.01.007.
Ceramicola, S., Praeg, D., Coste, M., Forlin, E., Cova, A., Colizza, E., Critelli, S., 2014. Submarine mass-movements along the slopes of the active Ionian continental margins and their consequences for marine geohazards (Mediterranean Sea). In: Submarine Mass Movements and their Consequences. Springer, pp. 295–306.
Civile, D., Zecchin, M., Tosi, L., Da Lio, C., Muto, F., Sandron, D., Mangano, G., 2022. The Petilia-Sosti Shear Zone (Calabrian Arc, southern Italy): an onshore-offshore regional active structure. Mar. Pet. Geol. 141, 105693.
Cohen, K.M., Finney, S.C., Gibbard, P.L., Fan, J.-X., 2013. Updated. The ICS International Chronostratigraphic Chart. Episodes 36, 199–204.
Consolaro, C., Macrì, P., Massari, F., Speranza, F., Fornaciari, E., 2013. A major change in the sedimentation regime in the Crotone Basin (Southern Italy) around 3.7–3.6 Ma. Palaeogeogr. Palaeoclimatol. Palaeoecol. 392, 398–410.
Corradino, M., Balazs, A., Faccenna, C., Pepe, F., 2022. Arc and forearc rifting in the Tyrrhenian subduction system. Scientific Rep. 12 (1), 4728. https://doi.org/10.1038/s41598-022-08562-w.
Corradino, M., Pepe, F., Bertotti, G., Picotti, V., Monaco, C., Nicolich, R., 2020. 3-D architecture and Plio-Quaternary evolution of the Paola Basin: Insights into the forearc of the Tyrrhenian-Ionian subduction system. Tectonics 39 (2) e2019TC005898.

Corradino, M., Pepe, F., Burrato, P., Kanari, M., Parrino, N., Bertotti, G., Bosman, A., Casalbore, D., Ferranti, L., Martorelli, E., Monaco, C., Sacchi, M., Tibor, G., 2021. An integrated multiscale method for the characterisation of active faults in offshore areas. The case of Sant'Eufemia Gulf (Offshore Calabria, Italy). Front. Earth Sci. 9, 670557. https://doi.org/10.3389/feart.2021.670557.

Cultrera, F., Barreca, G., Ferranti, L., Monaco, C., Pepe, F., Passaro, S., Scarfì, L., 2017. Structural architecture and active deformation pattern in the northern sector of the Aeolian-Tindari-Letojanni fault system (SE Tyrrhenian Sea-NE Sicily) from integrated analysis of field, marine geophysical, seismological and geodetic data. Ital. J. Geosci. 136 (3), 399–417.

De Ritis, R., Pepe, F., Orecchio, B., Casalbore, D., Bosman, A., Chiappini, M., Chiocci, F., Corradino, M., Nicolich, R., Martorelli, E., Monaco, C., Presti., D, Totaro, C., 2019. Magmatism along lateral slab edges: insights from the Diamante-Enotrio-Ovidio volcanic-intrusive complex (Southern Tyrrhenian Sea). Tectonics 38 (8), 2581–2605. https://doi.org/10.1029/2019TC005533.

Del Ben, A., Barnaba, C., Taboga, A., 2008. Strike-slip systems as the main tectonic features in the Plio-Quaternary kinematics of the Calabrian Arc. Mar. Geophys. Res. 29 (1), 1–12. https://doi.org/10.1007/s11001-007-9041-6.

Devoti, R., d'Agostino, N., Serpelloni, E., Pietrantonio, G., Riguzzi, F., Avallone, A., d'Ambrosio, C., 2017. A combined velocity field of the mediterranean region. Ann. Geophys. 60 (2) https://doi.org/10.4401/ag-7059.

DISS Working Group, . Database of Individual Seismogenic Sources (DISS), Version 3.2.1: A Compilation of Potential Sources for Earthquakes Larger Than M 5.5 in Italy and Surrounding Areas. Available at: http://diss.rm.ingv.it/diss/. Istituto Nazionale di Geofisica e Vulcanologia. https://doi.org/10.6092/INGV.IT-DISS3.2.1.

Faccenna, C., Becker, T.W., Lucente, F.P., Jolivet, L., Rossetti, F., 2001. History of subduction and back arc extension in the Central Mediterranean. Geophys. J. Int. 145 (3), 809–820.

Faccenna, C., Civetta, L., Antonio, M.D., Funiciello, F., Margheriti, L., Piromallo, C., 2005. Constraints on mantle circulation around the deforming Calabrian slab. Geophys. Res. Lett. 32 (6) https://doi.org/10.1029/2004GL021874.

Ferranti, L., Santoro, E., Mazzella, M.E., Monaco, C., Morelli, D., 2009. Active transpression in the northern Calabria Apennines, southern Italy. Tectonophysics 476 (1–2), 226–251. https://doi.org/10.1016/j.tecto.2008.11.010.

Ferranti, L., Burrato, P., Pepe, F., Santoro, E., Mazzella, M.E., Morelli, D., Vannucci, G., 2014. An active oblique-contractional belt at the transition between the Southern Apennines and Calabrian Arc: the Amendolara Ridge, Ionian Sea, Italy. Tectonics 33 (11), 2169–2194. https://doi.org/10.1002/2014TC003624.

Frepoli, A., Amato, A., 2000. Fault Plane Solutions of Crustal Earthquakes in Southern Italy (1988–1995): Seismotectonic Implications.

Galli, P.A.C., Peronace, E., 2015. Low slip rates and multimillennial return times for Mw 7 earthquake faults in southern Calabria (Italy). Geophys. Res. Lett. 42 (13), 5258–5265.

Guarnieri, P., 2006. Plio-Quaternary segmentation of the south Tyrrhenian forearc basin. Int. J. Earth Sci. 95 (1), 107–118. https://doi.org/10.1007/s00531-005-0005-2.

Gutscher, M.-A., Kopp, H., Krastel, S., Bohrmann, G., Garlan, T., Zaragosi, S., Le Faou, Y., 2017. Active tectonics of the Calabrian subduction revealed by new multibeam bathymetric data and high-resolution seismic profiles in the Ionian Sea (Central Mediterranean). Earth Planet. Sci. Lett. 461, 61–72.

Just, J., Hübscher, C., Betzler, C., Lüdmann, T., Reicherter, K., 2011. Erosion of continental margins in the Western Mediterranean due to sea-level stagnancy during the Messinian Salinity Crisis. Geo-Mar. Lett. 31, 51–64.

Knott, S.D., Turco, E., 1991. Late Cenozoic kinematics of the Calabrian arc, southern Italy. Tectonics 10 (6), 1164–1172.

Loher, M., Ceramicola, S., Wintersteller, P., Meinecke, G., Sahling, H., Bohrmann, G., 2018. Mud volcanism in a canyon: Morphodynamic evolution of the active Venere mud volcano and its interplay with Squillace Canyon, Central Mediterranean. Geochem. Geophys. Geosyst. 19 (2), 356–378.

Loreto, M.F., Fracassi, U., Franzo, A., Del Negro, P., Zgur, F., Facchin, L., 2013. Approaching the Seismogenic source of the Calabria 8 September 1905 earthquake: New Geophysical, Geological and Biochemical Data from the S. Eufemia Gulf (S Italy). Mar. Geol. 343, 62–75. https://doi.org/10.1016/j.margeo.2013.06.016.

Maesano, F.E., Tiberti, M.M., Basili, R., 2017. The Calabrian Arc: three-dimensional modelling of the subduction interface. Sci. Rep. 7 (1), 8887.

Mangano, G., Zecchin, M., Civile, D., Ceramicola, S., Donato, A., Muto, F., Critelli, S., 2022. Mid-Miocene to recent tectonic evolution of the Punta Stilo Swell (Calabrian Arc, southern Italy): an effect of Calabrian Arc migration. Mar. Geol. 448, 106810.

Massari, F., Prosser, G., 2013. Late Cenozoic tectono-stratigraphic sequences of the Crotone Basin: insights on the geodynamic history of the Calabrian arc and Tyrrhenian Sea. Basin Res. 25 (1), 26–51.

Massari, F., Prosser, G., Capraro, L., Fornaciari, E., Consolaro, C., 2010. A revision of the stratigraphy and geology of the south-western part of the Crotone Basin (South Italy). Ital. J. Geosci. 129 (3), 353–384.

Mattei, M., Cipollari, P., Cosentino, D., Argentieri, A., Rossetti, F., Speranza, F., Di Bella, L., 2002. The Miocene tectono-sedimentary evolution of the southern Tyrrhenian Sea: Stratigraphy, structural and palaeomagnetic data from the onshore Amantea basin (Calabrian Arc, Italy). Basin Res. 14 (2), 147–168. https://doi.org/10.1046/j.1365-2117.2002.00173.x.

Milia, A., Turco, E., Pierantoni, P.P., Schettino, A., 2009. Four-dimensional tectono-stratigraphic evolution of the Southeastern peri-Tyrrhenian basins (Margin of Calabria, Italy). Tectonophysics 476 (1–2), 41–56. https://doi.org/10.1016/j.tecto.2009.02.030.

Minelli, L., Billi, A., Faccenna, C., Gervasi, A., Guerra, I., Orecchio, B., Speranza, G., 2013. Discovery of a gliding salt-detached megaslide, Calabria, Ionian Sea, Italy. Geophys. Res. Lett. 40 (16), 4220–4224.

Molin, P., Dramis, F., Palmieri, E., 2002. The Pliocene-Quaternary uplift of the Ionian northern Calabria coastal belt between Corigliano Calabro and Capo Trionto. Studi Geol. Camerti Spec, 135–145.

Monaco, C., Tortorici, L., 2000. Active faulting in the Calabrian arc and eastern Sicily. J. Geodyn. 29 (3–5), 407–424.

Monaco, C., Tortorici, L., Nicolich, R., Cernobori, L., Costa, M., 1996. From collisional to rifted basins: an example from the southern Calabrian arc (Italy). Tectonophysics 266 (1–4), 233–249.

Monaco, C., Tortorici, L., Paltrinieri, W., 1998. Structural evolution of the Lucanian Apennines, southern Italy. J. Struct. Geol. 20 (5), 617–638.

Morelli, D., Cuppari, A., Colizza, E., Fanucci, F., 2011. Geomorphic setting and geohazard-related features along the Ionian Calabrian margin between Capo Spartivento and Capo Rizzuto (Italy). Mar. Geophys. Res. 32 (1), 139–149.

Neri, G., Orecchio, B., Totaro, C., Falcone, G., Presti, D., 2009. Subduction beneath southern Italy close the ending: results from seismic tomography. Seismol. Res. Lett. 80 (1), 63–70.

Neri, G., Orecchio, B., Scolaro, S., Totaro, C., 2020. Major Earthquakes of Southern Calabria, Italy, into the Regional Geodynamic Context. Front. Earth Sci. 8, 579846.

Patacca, E., Scandone, P., Crescenti, U., 2004. The Plio-Pleistocene thrust belt-foredeep system in the southern Apennines and Sicily (Italy). Geol. Italy 32, 93–129.

Pepe, F., Bertotti, G., Cella, F., Marsella, E., 2000. Rifted margin formation in the South Tyrrhenian Sea: a high-resolution seismic profile across the North Sicily passive continental margin. Tectonics 19, 241–257. https://doi.org/10.1029/1999TC900067.

Pepe, F., Sulli, A., Bertotti, G., Cella, F., 2010. Architecture and Neogene to recent evolution of the western Calabrian continental margin: an upper plate perspective to the Ionian subduction system, Central Mediterranean. Tectonics 29. https://doi.org/10.1029/2009TC002599. TC3007.

Pepe, F., Bertotti, G., Ferranti, L., Sacchi, M., Collura, A.M., Passaro, S., Sulli, A., 2014. Pattern and rate of post-20 ka vertical tectonic motion around the Capo Vaticano Promontory (W Calabria, Italy) based on offshore geomorphological indicators. Quat. Int. 332, 85–98.

Pirrotta, C., Barberi, G., Barreca, G., Brighenti, F., Carnemolla, F., De Guidi, G., Scarfì, L., 2021. Recent activity and Kinematics of the Bounding Faults of the Catanzaro Trough (Central Calabria, Italy): New Morphotectonic, Geodetic and Seismological Data. Geosciences 11 (10), 405.

Polonia, A., Torelli, L., Mussoni, P., Gasperini, L., Artoni, A., Klaeschen, D., 2011. The Calabrian Arc subduction complex in the Ionian Sea: Regional architecture, active deformation, and seismic hazard. Tectonics 30 (5).

Presti, D., Billi, A., Orecchio, B., Totaro, C., Faccenna, C., Neri, G., 2013. Earthquake focal mechanisms, seismogenic stress, and seismotectonics of the Calabrian Arc, Italy. Tectonophysics 602, 153–175.

Rosenbaum, G., Gasparon, M., Lucente, F.P., Peccerillo, A., Miller, M.S., 2008. Kinematics of slab tear faults during subduction segmentation and implications for Italian magmatism. Tectonics 27, 1–16. https://doi.org/10.1029/2007TC002143.

Rotondi, R., 2010. Bayesian nonparametric inference for earthquake recurrence time distributions in different tectonic regimes. J. Geophys. Res. Solid Earth 115 (B1).

Rovida, A., Locati, M., Camassi, R., Lolli, B., Gasperini, P., Antonucci, A., 2021. Parametric Catalogue of Italian Earthquakes CPTI15, Version 3.0.

Scarfì, L., Barberi, G., Barreca, G., Cannavò, F., Koulakov, I., Patanè, D., 2018. Slab narrowing in the Central Mediterranean: the Calabro-Ionian subduction zone as imaged by high resolution seismic tomography. Sci. Rep. 8 (1), 1–12.

Scarfì, L., Langer, H., Messina, A., Musumeci, C., 2021. Tectonic regimes inferred from clustering of focal mechanisms and their distribution in space: application to the Central Mediterranean Area. J. Geophys. Res. Solid Earth 126 (1) e2020JB020519.

Spadini, G., Cloetingh, S., Bertotti, G., 1995. Thermo-mechanical modeling of the Tyrrhenian Sea: Lithospheric necking and kinematics of rifting. Tectonics 14 (3), 629–644.

Spina, V., Tondi, E., Mazzoli, S., 2011. Complex basin development in a wrench-dominated back-arc area: tectonic evolution of the Crati Basin, Calabria, Italy. J. Geodyn. 51 (2–3), 90–109. https://doi.org/10.1016/j.jog.2010.05.003.

Tansi, C., Muto, F., Critelli, S., Iovine, G., 2007. Neogene-Quaternary strike-slip tectonics in the central Calabrian Arc (southern Italy). J. Geodyn. 43 (3), 393–414. https://doi.org/10.1016/j.jog.2006.10.006.

Totaro, C., Orecchio, B., Presti, D., Scolaro, S., Neri, G., 2016. Seismogenic stress field estimation in the Calabrian Arc region (South Italy) from a Bayesian approach. Geophys. Res. Lett. 43 (17), 8960–8969. https://doi.org/10.1002/2016GL070107.

Van Dijk, J.P., 1991. Basin dynamics and sequence stratigraphy in the Calabrian Arc (Central Mediterranean); records and pathways of the Crotone Basin. Geol. Mijnb. 70, 187–201.

Van Dijk, J.P., Scheepers, P.J.J., 1995. Neotectonic rotations in the Calabrian Arc; implications for a Pliocene-recent geodynamic scenario for the Central Mediterranean. Earth Sci. Rev. 39 (3–4), 207–246.

Van Dijk, J.P., Bello, M., Brancaleoni, G.P., Cantarella, G., Costa, V., Frixa, A., Zerilli, A., 2000. A regional structural model for the northern sector of the Calabrian Arc (southern Italy). Tectonophysics 324 (4), 267–320. https://doi.org/10.1016/S0040-1951(00)00139-6.

Volpi, V., Del Ben, A., Civile, D., Zgur, F., 2017. Neogene tectono-sedimentary interaction between the Calabrian Accretionary Wedge and the Apulian Foreland in the northern Ionian Sea. Mar. Pet. Geol. 83, 246–260. https://doi.org/10.1016/j.marpetgeo.2017.03.013.

Williams, G.D., Powell, C.M., Cooper, M.A., 1989. Geometry and kinematics of inversion tectonics. Geol. Soc. Lond., Spec. Publ. 44 (1), 3–15.

Zecchin, M., Accaino, F., Ceramicola, S., Civile, D., Critelli, S., Da Lio, C., Tosi, L., 2018. The Crotone Megalandslide, southern Italy: architecture, timing and tectonic control. Sci. Rep. 8 (1), 1–11.
Zecchin, M., Civile, D., Caffau, M., Critelli, S., Muto, F., Mangano, G., Ceramicola, S., 2020. Sedimentary evolution of the Neogene-Quaternary Crotone Basin (southern Italy) and relationships with large-scale tectonics: a sequence stratigraphic approach. Mar. Pet. Geol. 117, 104381.
Zhang, H., Thurber, C., Bedrosian, P., 2009. Joint inversion for vp, vs, and vp/vs at SAFOD, Parkfield, California. Geochem. Geophys. Geosyst. 10 (11).